

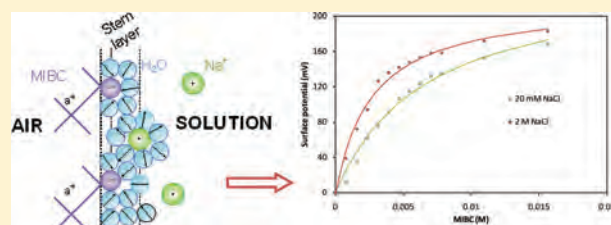
# Surface Potential of Methyl Isobutyl Carbinol Adsorption Layer at the Air/Water Interface

Chi M. Phan,<sup>\*,†</sup> Hiromichi Nakahara,<sup>‡</sup> Osamu Shibata,<sup>‡</sup> Yoshikiyo Moroi,<sup>‡</sup> Thu N. Le,<sup>†</sup> and Ha M. Ang<sup>†</sup>

<sup>†</sup> Department of Chemical Engineering, Curtin University, Perth WA 6845, Australia

<sup>‡</sup> Department of Biophysical Chemistry, Faculty of Pharmaceutical Sciences, Nagasaki International University, Sasebo, Nagasaki 859-3298, Japan

**ABSTRACT:** The surface potential ( $\Delta V$ ) and surface tension ( $\gamma$ ) of MIBC (methyl isobutyl carbinol) were measured on the sub-phase of pure water and electrolyte solutions (NaCl at 0.02 and 2 M). In contrast to ionic surfactants, it was found that surface potential gradually increased with MIBC concentration. The  $\Delta V$  curves were strongly influenced by the presence of NaCl. The available model in literature, in which surface potential is linearly proportional to surface excess, failed to describe the experimental data. Consequently, a new model, employing a partial charge of alcohol adsorption layer, was proposed. The new model predicted the experimental data consistently for MIBC in different NaCl solutions. However, the model required additional information for ionic impurity to predict adsorption in the absence of electrolyte. Such inclusion of impurities is, however, unnecessary for industrial applications. The modeling results successfully quantify the influence of electrolytes on surface potential of MIBC, which is critical for froth stability.



## 1. INTRODUCTION

Alcohols are amphiphilic molecules and can strongly absorb into the air/liquid interface. Practically, alcohols, including branched- and short-chained ones, have been used extensively in industrial processes to enhance the interfacial effect. For example, the alkanols with 5 to 8 carbons<sup>1</sup> have been applied as a frother to stabilize small air bubbles in mineral flotation. Similarly, 2-ethyl-hexanol has been used as a heat transfer additive in steam condensation.<sup>2</sup> Among these aliphatic alkanols, MIBC (methyl isobutyl carbinol) is particularly interested due to the superior performance in mineral flotation. The interfacial behavior of MIBC at the air/liquid interface has been investigated employing foamingness,<sup>3,4</sup> thin aqueous film,<sup>5–7</sup> and zeta-potential.<sup>5,8</sup> Nevertheless, the mechanism for frothability induced by MIBC remains not well-understood. In particular, the surface potential ( $\Delta V$ ), which directly influences the double-layer force and disjoining pressure, has not been investigated.

In the present study, MIBC surface adsorption from the aqueous solutions with and without NaCl is investigated by surface tensiometry ( $\gamma$ ) and surface potential ( $\Delta V$ ).

## 2. THEORETICAL MODEL

There are a number of proposed models for surface adsorption at the air/water interface, which are based on the surface tension and surface potential of surfactants.<sup>9–11</sup> Most of these models focused on ionic surfactants, which involve the interfacial adsorption of their counterions. Although fitting experimental data well, these models require a number of parameters, which cannot be verified independently.

In this study, the surface adsorption model was modified and applied to nonionic surfactants. More critically, coordinated experiments were

selected to limit the number of fitting parameters and improve the reliability of modeling.

The main principle of our model is presented in Figure 1. Instead of neutral charge as often assumed in the literature, the model assumes a small negative charge at the hydroxyl group due to the polarity of the alcohol. The adsorption of alcohols leads to the formation of the electric double layer at the air/solution interface. The hydroxyl group, which is negatively charged, forms a charged layer at the interface in the Stern layer. Hydrated cations in the Stern layer can be shared by several hydroxyl groups as suggested by Warszyński and coauthors.<sup>11</sup> The cations in the diffuse part can approach the interface at the distance as equal to the thickness of the Stern layer.

The surface potential of the MIBC solution was determined relatively to the surface potential of the pure solvent or supporting electrolyte

$$\Delta V = V_a - V_0 \quad (1)$$

where  $V_a$  is the surface potential measured in the presence of alcohol, and  $V_0$  is the potential measured in the absence of alcohol (either pure water or electrolyte solutions).

The change in surface potential due to the presence of adsorbed MIBC molecules is given as<sup>11</sup>

$$\Delta V = N_A \Gamma_a \frac{\mu^t}{\epsilon_a \epsilon_0} + \sigma \frac{\lambda_s}{\epsilon_s \epsilon_0} + \psi_d \quad (2)$$

where

**Received:** October 19, 2011

**Revised:** December 15, 2011

**Published:** December 15, 2011

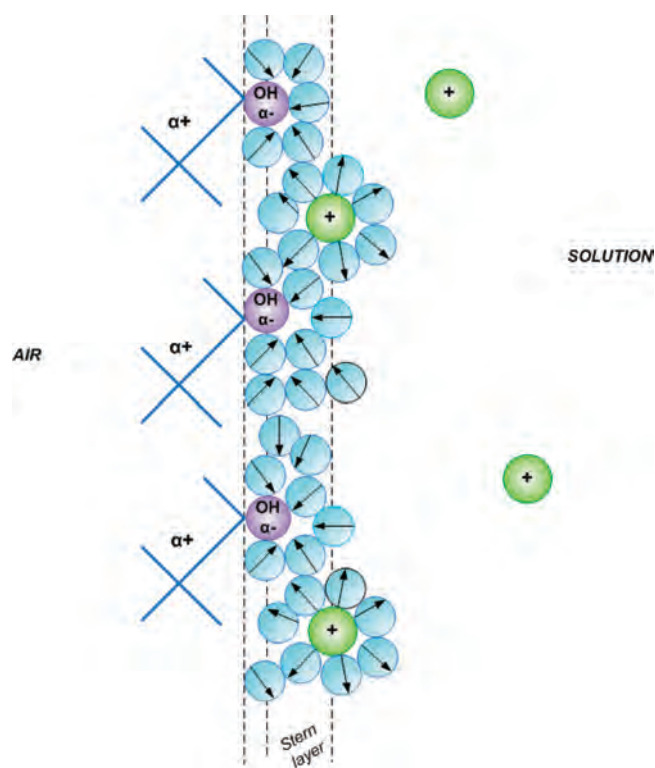


**Figure 1.** Proposed surface adsorption model for MIBC in this study.

$\epsilon_0$  is vacuum permittivity,

$\epsilon_a$  and  $\epsilon_s$  are dielectric permittivity of the adsorbed layer and Stern layer, respectively,

$\Gamma_a$  is the surface concentration of alcohol,

$\mu^t$  is the total normal dipole moment per MIBC molecules, which consists of the (i) dipole moment of adsorbed alcohol and the (ii) dipole moment of water molecules disordered by alcohols,<sup>11,12</sup>

$\sigma$  is the surface charge density,

$\psi_d$  is the potential at the limit of the diffuse layer, and

$\lambda_s$  is thickness of the Stern layer.

In eq 1, the first term accounts for the dipole moment of the adsorption layer, the second term accounts for the potential across the Stern layer, and the third term accounts for the potential from the Stern layer to infinity (inside the bulk).

It should be noted that  $\epsilon_a < \epsilon_s < \epsilon$ , where  $\epsilon$  is the dielectric permittivity of water. For a short alcohol such as MIBC, it can be assumed that the  $\mu^t$  is independent of  $\Gamma_a$ .<sup>11</sup> For monovalent electrolytes, the third term in eq 1 can be related to the surface charge by the Grahame equation<sup>13</sup>

$$\sigma = \sqrt{8 \times 10^3 c_{\text{cation}} N_A \epsilon \epsilon_0 k_B T} \sinh\left(\frac{e\psi_d}{2k_B T}\right) \quad (3)$$

where  $c_{\text{cation}}$  is the effective cation concentration, which also equals the anion concentration in the bulk.

It is well-known that pure water can dissociate itself into hydronium ( $\text{H}_3\text{O}^+$ ) and hydroxide ( $\text{OH}^-$ ),<sup>14</sup> albeit at very low concentration ( $\sim 2 \times 10^{-7}$  M). Recently, experimental (vibrational sum frequency generation spectroscopy) and molecular dynamics studies have revealed that protonated water exists in the interfacial region due to the hydrophobic nature of the oxygen in hydronium.<sup>15</sup> Similarly, a comparative second harmonic

generation study also demonstrates an enhanced concentration of protonated water at the interface region.<sup>16</sup> Consequently,  $c_{\text{cation}}$  is always nonzero, even in the absence of electrolyte. Practically, MIBC solutions may have a certain ionic strength due to the ionic impurities in MIBC.

The surface charge density at the boundary between diffuse layer and Stern layer is given as

$$\sigma = eN_A \Gamma_{\text{cation}} \quad (4)$$

where  $\Gamma_{\text{cation}}$  is the adsorbed concentration of the cation at the interface due to the MIBC adsorption. Within the Stern layer arrangement, the partially charged hydroxyl group of MIBC is assumed to be thermodynamically balanced by a certain number of cations, and therefore

$$\Gamma_{\text{cation}} = \alpha \Gamma_a \quad (5)$$

where  $\alpha$  is the effective charge of the hydroxyl group,  $\alpha < 1$  (Figure 1).

Combining eqs 2, 3, and 4, the relative surface potential is given by

$$\Delta V = N_A \Gamma_a \frac{\mu^t}{\epsilon_a \epsilon_0} + \alpha e N_A \Gamma_a \frac{\lambda_s}{\epsilon_s \epsilon_0} + \frac{2k_B T}{e} \operatorname{arcsinh}\left(\frac{\alpha e N_A \Gamma_a}{\sqrt{8 \times 10^3 c_{\text{cation}} N_A \epsilon \epsilon_0 k_B T}}\right) \quad (6)$$

The equation can be simplified by introducing a combined parameter

$$\beta = \frac{\mu^t}{\epsilon_a \epsilon_0} + \alpha e \frac{\lambda_s}{\epsilon_s \epsilon_0} \quad (7)$$

In this instance,  $\beta$  is a parameter independent of  $\Gamma_a$ . Consequently, eq 6 reduces to

$$\Delta V = N_A \Gamma_a \beta + \frac{2k_B T}{e} \operatorname{arcsinh}\left(\frac{\alpha e N_A \Gamma_a}{\sqrt{8 \times 10^3 c_{\text{cation}} N_A \epsilon \epsilon_0 k_B T}}\right) \quad (8)$$

Generally, eq 8 requires three unknown parameters:  $\alpha$ ,  $\beta$ , and  $c_{\text{cation}}$ . However, in the presence of strong electrolytes such as NaCl,  $c_{\text{cation}}$  is determined by the electrolyte concentration, and thus, only two parameters are needed. In the new model, the cation size only affects  $\beta$  (since the Stern layer thickness depends on hydrated cation size), not  $\alpha$ .

The new model, eq 8, is actually a general case of available models in the literature. When  $\alpha = 1$ , this equation reduces to the adsorption model for anionic surfactants.<sup>17</sup> When  $\alpha = 0$ , eq 8 reduces to a linear form as proposed by Warszyński and coauthors for nonionic surfactants<sup>11</sup>

$$\Delta V = N_A \Gamma_a \frac{\mu^t}{\epsilon_a \epsilon_0} \quad (9)$$

Qualitatively, there are two distinguishing differences between eqs 8 and 9.

- (1) The relationship between surface excess and surface potential: eq 9 gives a linear relationship, whereas eq 8 yields a nonlinear relationship.
- (2) The influence of the type of ionic species, for example,  $\text{Na}^+$  and  $\text{H}_3\text{O}^+$ , on the relationship between surface

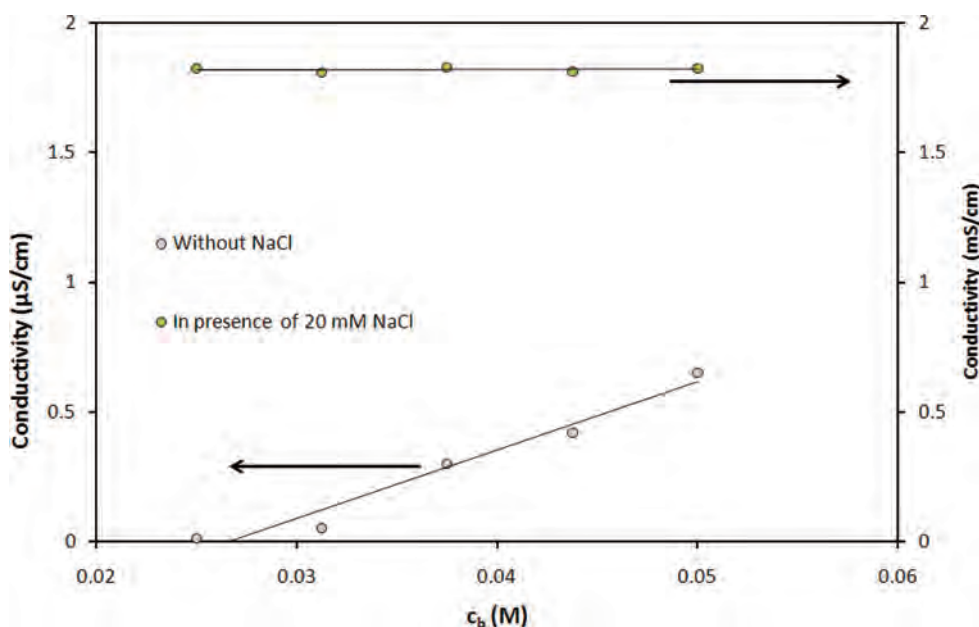


Figure 2. Conductivity as function of MIBC concentration, with and without NaCl.

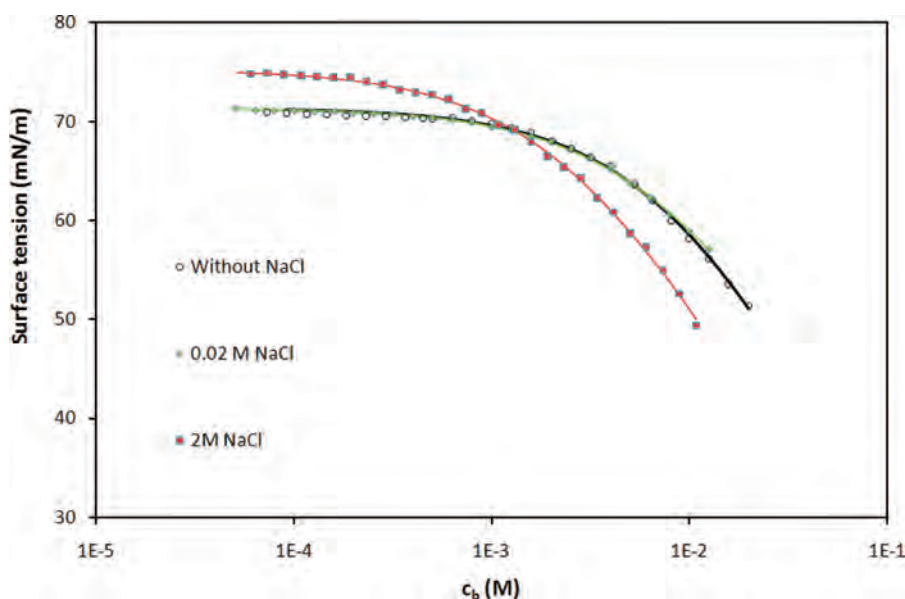


Figure 3. Surface tension of MIBC with and without NaCl (dots, experimental data; lines, modeled prediction).

excess and surface potential: eq 9 gives the same straight line, whereas eq 8 gives different curves.

Finally, the adsorption excess of alcohol is determined by surface tension in combination with a Langmuir isotherm

$$c_b = \frac{1}{K} \left( \frac{\Gamma_a}{\Gamma_m - \Gamma_a} \right) \quad (10)$$

Where  $K$  and  $\Gamma_m$  are adsorption constants that can be found by fitting surface tension to the Szyszkowski equation<sup>18</sup>

$$\gamma_0 - \gamma_a = -RT\Gamma_m \ln(1 + Kc_b) \quad (11)$$

where  $\gamma_0$  and  $\gamma_a$  are surface tension of alcohol-free (pure solvent or supporting solute) and alcohol solutions, respectively.

In applying eq 11, the Gibbs energy of supporting electrolytes adsorption is assumed independent to alcohol adsorption as proposed by Karraker and Radke,<sup>10</sup> whereas the surface energy accounting for the adsorbed cations, i.e.,  $\Gamma_{\text{cation}}$  in the Stern layer is ignored. This assumption will be justified later. Since MIBC does not form micelles, unlike ionic surfactants, the Gibbs isotherm and eq 11 can be applied for MIBC concentrations below solubility.

### 3. EXPERIMENTAL SECTION

**3.1. Surface Tension ( $\gamma$ ).** The experimental setup consisted of the Wilhelmy plate method,<sup>19</sup> using a KSV Sigma 701 tensiometer cooperated with an automatic microdispenser. The Wilhelmy plate is made of platinum with the periphery of 39.4 mm.

**3.2. Conductivity ( $\kappa$ ).** The conductivity of MIBC was measured at 5 different concentrations with and without NaCl using a TPS-WWP-81 conductivity meter. The NaCl concentration was selected at 0.02 M.

**3.3. Surface Potential ( $\Delta V$ ).** The surface potential of the MIBC solution was determined relative to the surface potential of the pure supporting electrolyte (water; 0.02 and 2 M of NaCl) using an ionizing  $^{241}\text{Am}$  electrode. Details of surface potential measurements have been described elsewhere.<sup>12,20</sup>

## 4. RESULTS

**4.1. Conductivity.** The conductivity of MIBC in pure water and 0.02 M NaCl are plotted in Figure 2. It can be seen that MIBC linearly increased the conductivity from 0 to  $0.65 \mu\text{S}/\text{cm}$ , which indicates some ionic impurities. In presence of 0.02 M NaCl, however, the conductivity was strongly dominated by NaCl and independent of MIBC concentration ( $\sim 1821 \pm 8 \mu\text{S}/\text{cm}$ ). Hence, the proposed model can be applied for MIBC solution in NaCl solutions, at both 0.02 and 2 M. However, the addition equation is required to account for ionic impurity in the absence of NaCl.

**4.2. Surface Tension.** The surface tension ( $\gamma$ ) of MIBC in water and NaCl solutions were fitted to eq 11 by the least-squares

**Table 1. Best-Fitted Parameters for Surface Tension and Surface Potential<sup>a</sup>**

	surface tension (eq 11)			surface potential (eq 9)	
	$K$ ( $\text{M}^{-1}$ )	$\Gamma_m$ ( $\times 10^6 \text{ mol}/\text{m}^2$ )	$\delta$ ( $\text{mN}/\text{m}$ )	slope ( $\text{Vm}^2$ )	$\delta$ ( $\text{mV}$ )
water	100.4	7.47	0.257	$5.64 \times 10^7$	15.0
0.02 M NaCl	139.7	5.71	0.091	$4.48 \times 10^7$	6.3
2 M NaCl	369.0	6.36	0.242	$3.42 \times 10^7$	5.5

<sup>a</sup>The standard deviations are calculated by

$$\delta = \sqrt{\frac{\sum_{i=1}^n (x_{i,\text{exp}} - x_{i,\text{modelled}})^2}{n}} \quad (12)$$

where  $n$  is the number of experimental data.

method, using  $K$  and  $\Gamma_m$  as adjustable parameters. Since there are many local best-fitted points for the Szyszkowski equation, different initial guesses were used to fit the surface tension data to eq 11. Consequently, the smallest standard deviation was selected.

The surface tension ( $\gamma$ ) data and best-fitted curves are plotted in Figure 3. It can be seen that the data for pure water and 0.02 M NaCl are almost overlapping. However, the high NaCl solution had higher surface tension ( $75.29 \text{ mN}/\text{m}$ ). The results are consistent with other data in the literature.<sup>21</sup> Applying the surface tension model, the best-fitted value of  $\Gamma_m$  is within the typical range for nonionic surfactants, albeit at the lower end due to bulky structure (Table 1). However, the best-fitted value of  $K$  varied significantly. The behaviors of  $K$  and  $\Gamma_m$  in different salinity are similar to modeling results of SDS in NaCl as reported by Prosser and Franses.<sup>22</sup> It should be noted that all standard deviations were smaller than  $1 \text{ mN}/\text{m}$ , which is the proposed threshold for good fitting.

**4.3. Surface Potential.** In contrast to cationic and anionic surfactants,<sup>20</sup> the surface potential ( $\Delta V$ ) of MIBC demonstrated a continuous increment with concentration. To verify the new model, the existing model, eq 9, was first applied to three surface potential data (with best-fitted slopes tabulated in Table 1). Subsequently, the new model was applied to electrolyte solutions simultaneously. Finally, the new equation with an additional equation accounting for ionic impurities was applied to MIBC in pure water.

**4.3.1. Existing Model.** The existing model, eq 9, was applied to three data individually. To highlight the nonlinear relationship, the surface potential of MIBC were also plotted against the surface excess (Figure 4). It can be seen (from Figure 4 and Table 1) that the modeled slopes of linear lines are different from pure water to NaCl solutions, which indicate the influence of cations on the potential constant. The slopes between two NaCl solutions were also significantly different. From these results, it can be concluded that the nature and concentration of the ion have a significant influence on adsorption of MIBC at the air/water interface.

**4.3.2. New Model for Electrolyte Solutions.** The new model was applied to surface potential data in the presence of NaCl, at

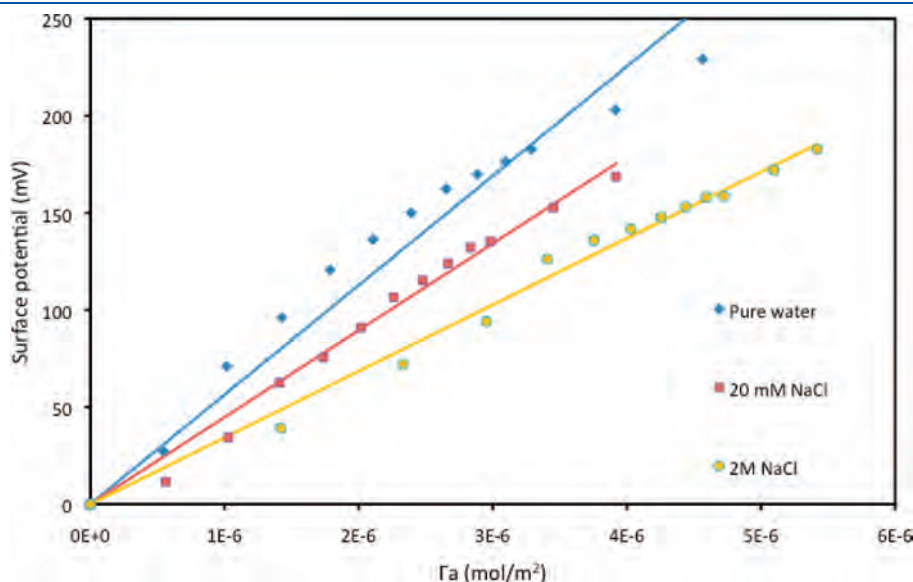


**Figure 4.** Linear predictions, eq 9, for the surface potential of MIBC on the different subphases.

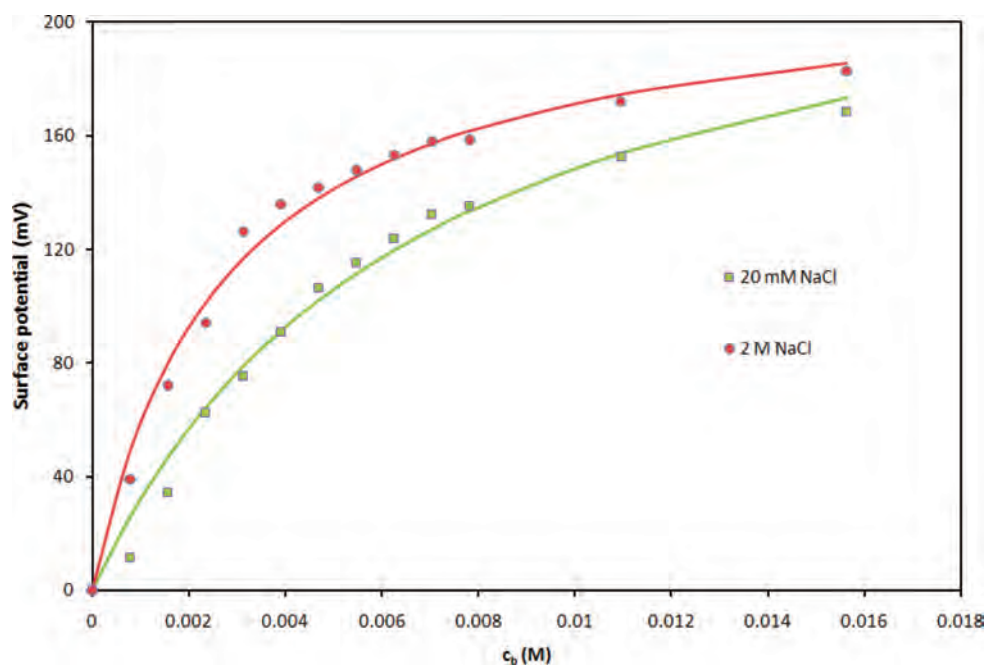


**Figure 5.** Surface potential of MIBC on the NaCl aqueous solutions (points, experimental data; lines, modeled predictions). The best-fitted values of parameters are  $\alpha = 0.043$  and  $\beta = 3.3 \times 10^4 \text{ Vm}^2$  ( $\delta = 6 \text{ mV}$ ).

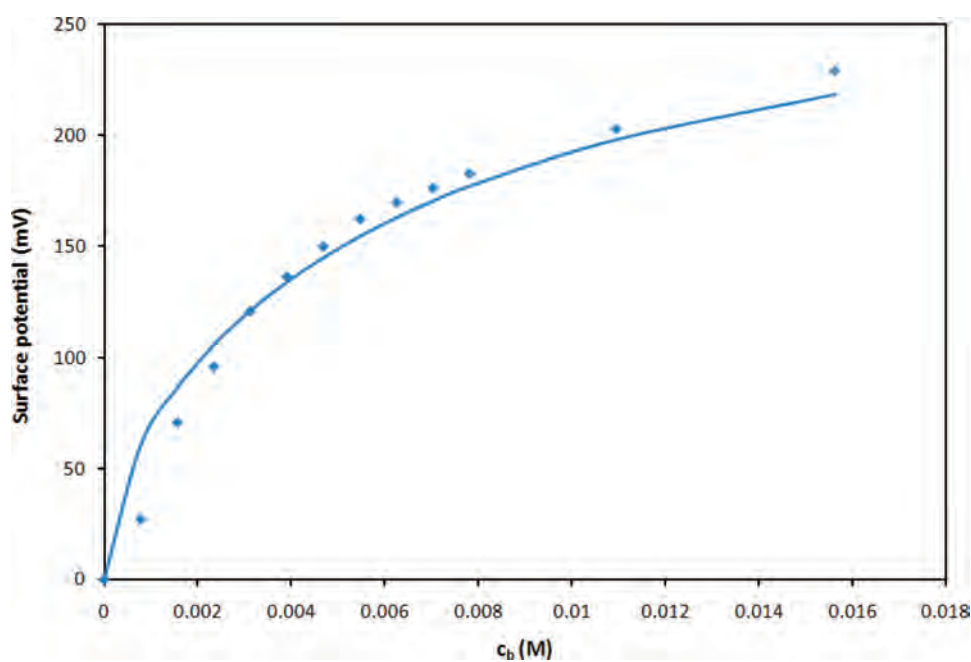


**Figure 6.** Surface potential of MIBC on water; line, best-fitted curve  $\nu = 0.53$  and  $\delta = 11.7 \text{ mV}$ .

both 0.02 and 2 M. Since  $\alpha$  and  $\beta$  in eq 8 are independent of NaCl concentration, the model was fitted against data at both concentrations simultaneously (using least sum of squares method with MS Excel Solver). As shown in Figure 5, the model fits both data consistently (with overall standard deviation of 6 mV). It is noteworthy that the fitting in Figure 5 was independent of the initial guesses of  $\alpha$  and  $\beta$ . When fitting to the curves individually, on the contrary, the best-fitted values vary with initial guesses, and there are different best-fitted combinations of  $\alpha$  and  $\beta$  (results are not shown).

**4.3.3. Modeling Surface Potential of MIBC in Pure Water.** For MIBC in water, an additional equation is required to account for ionic impurity. If self-dissociation of water is neglected, the ionic concentration of MIBC solution is linearly dependent on MIBC concentration and given as

$$c_{\text{cation}} = \nu c_b \quad (13)$$

where  $\nu$  is the percentage of ionic impurity.

**Table 2. Physical Parameters Satisfying the Modeling Parameters**

parameters	set 1	set 2	typical range
$\mu^{\dagger}/\varepsilon_a$ (D)	0.138	0.134	0.19–0.22 for SDS <sup>11</sup>
$\lambda_S$ (Å)	1.0	1.6	comparable to ionic radius
$\varepsilon_s$	30	30	recommended by Schuhmann <sup>26</sup>

If the impurity is assumed to be univalent ions, eq 13 can be combined with eq 8 to predict the surface potential of MIBC in pure water. The modeled prediction is fitted to the experimental data by adjusting  $\nu$  (Figure 6). It can be seen that the model predicted data reasonably well, albeit with a very large impurity. The unrealistic value of impurity can be contributed to the univalent ion assumption. For a multicationic system with higher valence, the effective cation concentration is given as

$$c_{\text{cation}} = \sum_i c_i^0 z_i^2 \quad (14)$$

where  $z_i$  is the valency of  $i$ th cation sort.

In multi-ions systems, the effective anionic concentration can be different to cation concentration, and a revised Grahame equation is needed. Moreover, the ionic concentration can also be influenced by dissociation of water and MIBC. Surface dissociation of nonionic surfactant has been reported in the literature.<sup>23</sup> Consequently, an appropriate model for MIBC in pure water is only derivable if the nature and composition of ionic impurity is known. For industrial applications, however, such inclusion of impurity is unnecessary. Mineral flotation, for instance, always employs in medium to high ionic strength due to mineral particles, ionic agents, and usage of water without deionization. In such cases, the ionic strength is always dominated by these ions, and the ionic impurities are negligible.

## 5. DISCUSSION

The partial charge obtained from modeling,  $\alpha$ , should be smaller than the total charge of hydroxyl group obtained from molecular dynamics: 0.265<sup>24</sup> or 0.160.<sup>25</sup> Since the effective charge of the alcohol hydrophilic head should also be influenced by the charge of  $\alpha$ -carbon, a partial charge of 0.04 is physically plausible.

To justify the best-fitted value of  $\beta$ , one needs to solve eq 3. Because of a large number of independent parameters, however, there could be numerous combinations to match the values of  $\alpha$  and  $\beta$ . Examples of combinations are tabulated in Table 2. It should be noted that both combinations are agreed with literature values and  $\varepsilon_s < \varepsilon$ . Hence, it can be concluded that the best-fitted values of both  $\alpha$  and  $\beta$  are physically feasible.

Finally, the contribution of  $\Gamma_{\text{cation}}$  on the surface tension is reconsidered to justify model assumption. The Gibbs free energy of the electric double layer per unit area is given by<sup>13</sup>

$$\Delta g = -\sqrt{8 \times 10^3 c_{\text{cation}} N_A \varepsilon \varepsilon_0 k_B T \frac{2k_B T}{e}} \left[ \cosh\left(\frac{e\psi_d}{2k_B T}\right) - 1 \right] \quad (15)$$

By applying the above equation at the highest concentration of MIBC in 0.02 M NaCl ( $\psi_d = 44$  mV), the Gibbs energy of adsorbed cations is 0.33 mN/m, which is negligible in comparison to surface tension in Figure 3. Consequently, it can be concluded that the model assumption remains valid.

## 6. CONCLUSIONS

The surface potential ( $\Delta V$ ) and surface tension ( $\gamma$ ) of MIBC was measured in water and electrolyte solutions (NaCl at 0.02 and 2 M). In contrast to ionic surfactants, it was found that the surface potential gradually increased with MIBC concentration. The  $\Delta V$  curves were strongly influenced by the presence of NaCl. The available model in literature, in which surface potential is linearly proportional to surface excess, cannot describe the experimental data. Consequently, a new model, which employed a nonzero charge of alcohol, was applied. The proposed model described the experimental data consistently for MIBC in electrolyte solutions. The best-fitted values of two fitting parameters are physically feasible. To predict MIBC in pure water, however, the model framework requires additional information regarding ionic impurity and/or self-dissociation of alcohol. Nevertheless, such information is unnecessary for commercial applications due to the high ionic strength of solvent in industrial processes.

The modeling results successfully quantify the influence of electrolytes on surface potential of frother solutions, which directly underpin the double-layer forces and froth stability. The new model is also applicable to other aliphatic alcohols, which are widely used in industrial processes. Further study, such as molecular dynamics, is recommended to quantify the influence of molecular structure on partial charges and interfacial adsorption of frothers.

## AUTHOR INFORMATION

### Corresponding Author

\*E-mail: c.phan@curtin.edu.au.

## REFERENCES

- Klimpel, R. R. *Int. J. Miner. Process.* **1991**, *33*, 369.
- Jun, Y.-D.; Kim, K. J.; Kennedy, J. M. *Int. J. Refrig.* **2010**, *33*, 428.
- Comley, B. A.; Harris, P. J.; Bradshaw, D. J.; Harris, M. C. *Int. J. Miner. Process.* **2002**, *64*, 81.
- Tan, S. N.; Pugh, R. J.; Fornasiero, D.; Sedev, R.; Ralston, J. *Miner. Eng.* **2005**, *18*, 179.
- Qu, X.; Wang, L.; Karakashev, S. I.; Nguyen, A. V. *J. Colloid Interface Sci.* **2009**, *337*, 538.
- Wang, L.; Yoon, R.-H. *Int. J. Miner. Process.* **2008**, *85*, 101.
- Karakashev, S. I.; Ivanova, D. S.; Angarska, Z. K.; Manev, E. D.; Tsekov, R.; Radoev, B.; Slavchov, R.; Nguyen, A. V. *Colloids Surf., A* **2010**, *365*, 122.
- Elmahdy, A. M.; Mirnezami, M.; Finch, J. A. *Int. J. Miner. Process.* **2008**, *89*, 40.
- Karakashev, S.; Nguyen, A.; Miller, J. Equilibrium Adsorption of Surfactants at the Gas–Liquid Interface. In *Interfacial Processes and Molecular Aggregation of Surfactants*; Narayanan, R., Ed.; Springer: Berlin/Heidelberg, Germany, 2008; Vol. 218, p 25.
- Karraker, K. A.; Radke, C. J. *Adv. Colloid Interface Sci.* **2002**, *96*, 231.
- Warszyński, P.; Barzyk, W.; Lunkenheimer, K.; Fruhner, H. *J. Phys. Chem. B* **1998**, *102*, 10948.
- Nakahara, H.; Shibata, O.; Rusdi, M.; Moroi, Y. *J. Phys. Chem. C* **2008**, *112*, 6398.
- Butt, H.-J.; Graf, K.; Kappl, M. *The Electric Double Layer. In Physics and Chemistry of Interfaces*; Wiley-VCH Verlag GmbH & Co. KGaA: New York, 2004; p 42.
- Zimmermann, R.; Freudenberg, U.; Schweiß, R.; Küttner, D.; Werner, C. *Curr. Opin. Colloid Interface Sci.* **2010**, *15*, 196.
- Mucha, M.; Frigato, T.; Levering, L. M.; Allen, H. C.; Tobias, D. J.; Dang, L. X.; Jungwirth, P. *J. Phys. Chem. B* **2005**, *109*, 7617.
- Petersen, P. B.; Saykally, R. J. *J. Phys. Chem. B* **2005**, *109*, 7976.

- (17) Manev, E. D.; Sazdanova, S. V.; Tsekov, R.; Karakashev, S. I.; Nguyen, A. V. *Colloids Surf., A* **2008**, *319*, 29.
- (18) Chang, C. H.; Franses, E. I. *Colloids Surf., A* **1995**, *100*, 1.
- (19) Barnes, G.; Gentle, I. *Interfacial Science*; Oxford University Press: Oxford, U.K., 2005.
- (20) Nakahara, H.; Shibata, O.; Moroi, Y. *J. Phys. Chem. B* **2011**, *115*, 9077.
- (21) Ozdemir, O.; Karakashev, S. I.; Nguyen, A. V.; Miller, J. D. *Miner. Eng.* **2009**, *22*, 263.
- (22) Prosser, A. J.; Franses, E. I. *Colloids Surf., A* **2001**, *178*, 1.
- (23) Maltseva, E.; Shapovalov, V. L.; Möhwald, H.; Brezesinski, G. *J. Phys. Chem. B* **2005**, *110*, 919.
- (24) Jorgensen, W. L. *J. Phys. Chem.* **1986**, *90*, 1276.
- (25) Gao, J.; Habibollahzadeh, D.; Shao, L. *J. Phys. Chem.* **1995**, *99*, 16460.
- (26) Schuhmann, D. *J. Colloid Interface Sci.* **1990**, *134*, 152.